Journal of Minerals and Materials Characterization and Engineering, 2023, 11, 81-91
https://www.scirp.org/journal/jmmce
ISSN Online: 2327-4085
ISSN Print: 2327-4077

Physic, Chemical and Mineralogical Characterizations of Clays Used in the Making of Traditional Ceramics in the City of Katiola, Côte d'Ivoire

Isabelle Linda He[1], Grah Patrick Atheba[2,3*], N'guadi Blaise Allou[2], Patrick Drogui[3], My Ali El Khakani[4], Gildas Komenan Gbassi[1]

[1]Laboratory of Analytical Sciences and Public Health, Training and Research Unit of Pharmaceutical Sciences and Biological, University Félix Houphouët Boigny, Abidjan, Côte d'Ivoire
[2]Laborararatory of Constitution and Reaction of Matter, Unit for Training and Research in the Sciences of the Structures of Matter and Technology, University Félix Houphouët Boigny, Abidjan, Côte d'Ivoire
[3]Center Water Earth Environment, National Institute for Scientific Research, Quebec, Canada
[4]Center Energy, Materials and Telecommunications, National Institute for Scientific Research, Varennes, Canada
Email: *grahpatrick.atheba@gmail.com

How to cite this paper: He, I.L., Atheba, G.P., Allou, N.B., Drogui, P., El Khakani, M.A. and Gbassi, G.K. (2023) Physic, Chemical and Mineralogical Characterizations of Clays Used in the Making of Traditional Ceramics in the City of Katiola, Côte d'Ivoire. *Journal of Minerals and Materials Characterization and Engineering*, **11**, 81-91.
https://doi.org/10.4236/jmmce.2023.114008

Received: April 21, 2023
Accepted: July 28, 2023
Published: July 31, 2023

Abstract

In Côte d'Ivoire, traditional ceramics are widely used in the form of pottery. The latter is used to store food, water and cereals. Analyzes (X-ray diffraction (XRD), Fourier transform infrared spectroscopy (FTIR), inductive plasma optical emission spectrometry (ICP-OES), scanning electron microscopy (SEM) and analysis thermal gravimetric (ATG)) were carried out to determine the morphology, the chemical, physical and pedological constituents of these raw materials. It appears from this study that the clays used in the Mangoro pottery of Katiola contain silica SiO_2, alumina Al_2O_3 and iron oxide Fe_2O_3 as well as kaolinite, muscovite, smectite and quartz.

Keywords

Ceramics, Characterization, Clays, Kaolinite, Muscovite, Smectite, Quartz

1. Introduction

In Côte d'Ivoire, traditional ceramics are widely used in the form of pottery. Potteries are used for drinking water storage, cereals conservation, food cooking and also as dishes [1]. Pottery belongs to artistic craftsmanship, and that of Katiola, made by the Mangoro women, remains the most famous in the country [2]. Clay materials used for Katiola pottery remain scientifically unknown. Only a

few publications are available in the literature [3] [4]. In order to characterize and identify clays used in Mangoro pottery, clay samples collected in the clearings exploited by the craftsmen were treated and analyzed by classical analytical methods for the characterization of clay minerals [5]. X-ray diffraction (XRD) allows the identification of the nature and structure of crystallized compounds. It is used preferentially in the mineralogical characterization of clay materials [6]. Fourier transform infrared (FTIR) spectroscopy is performed in addition to XRD [7]. Inductive plasma optical emission spectrometry (ICP-OES) is applied to determine the composition of major mineral elements [8] [9]. Scanning electron microscopy (SEM) gives, at a resolution scale less than one micrometer, the shape, precise size and texture of materials surfaces [6] [8]. Thermal gravimetric analysis is important because it locates the essential transformations that are dehydration, dehydroxylation and recrystallization of the materials [6].

The present work aims to determine the physical, chemical and mineralogical characteristics (ICP-OES, DRX, FTIR, and SEM) of the raw clay materials used in traditional ceramics of Katiolacity.

2. Materials and Methods

2.1. Sampling

Clay samples studied were collected from Katiola (**Figure 1**) in Côte d'Ivoire (GPS coordinates: Altitude 326 m; Latitude N 8˚08'14"; Longitude O 5˚06'03"). Seven samples were collected from the extraction site. They are codified from K1 to K7.

2.2. pH Determination

10% clay solution (10 g of clay powder in 100 ml of distilled water) was stood for 24 hours (time required for the dissolution of the mineral elements). When measuring the pH, the solution is homogenized using a magnetic stirrer for 10 minutes. The reading was done directly using HANNA pH meter [7].

2.3. Materials Characterization

2.3.1. ICP-OES Analysis

The concentrations of metals and elements were measured by inductively coupled plasma optical emission spectroscopy (ICP-OES) on a Varian apparatus (St-Laurent, Canada), model Vista Ax. A solution of cesium chloride (to improve atomization) and yttrium (1 mg/l) as an internal standard was mixed with the sample. A certified control solution (ICP-OES & ICP-MS standard) PlasmaCal Multielement Standard 900-Q30-100 (SCP Sciences, Baie-D'Urfé, Quebec, Canada) was used to ensure the accuracy of the analyses.

2.3.2. X-Ray Diffraction Analysis

X-ray diffraction (XRD) was performed to reveal information about the structure of the analyzed powders. For this, a D8 Advance diffractometer (Bruker) with an X-ray source (copper anticathode Kα1 (λ = 1.5406 Å) and Kα2 (λ =

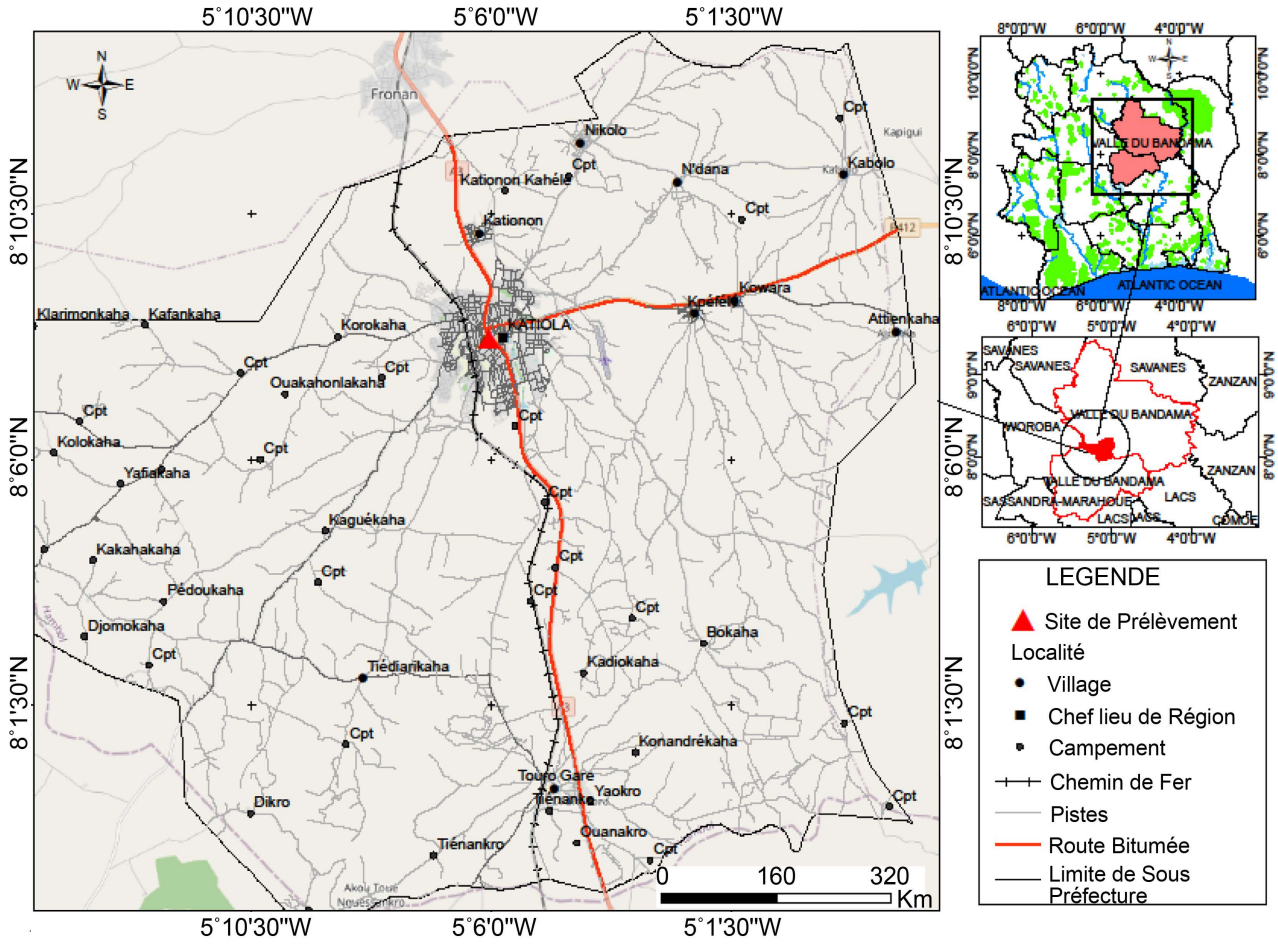

Figure 1. Map location of sampling area.

1.5445 Å)) is used. The measurements were taken in the Bragg-Brentano θ/θ configuration. The K powder samples were analyzed over a range of 2θ angles between 5˚ and 60˚ with a scan rate of 0.04˚.

2.3.3. Fourier Transform Infrared (FT-IR) Analysis

Analysis by Fourier Transform Infrared Spectroscopy (FT-IR) is used to study the type of bonds formed within materials. All the K powder samples were mixed separately with potassium bromide powder (KBr, Fisher Chemical) in order to obtain a ratio of 1% mass of K powder mixed with the KBr and for a total mass of 0.2 g per sample. This mixture of K and KBr powder is first ground using a pestle and mortar to ensure the homogeneity of the mixture. The latter is then pressed in the form of pellets ~1 cm in diameter using a manual press. The FT-IR analyses of the different K powders were carried out using a Nicolet 6700 spectrometer (Thermo Electron) in absorbance mode. The FT-IR measurements were made with a spectral resolution of 4 cm^{-1} over the spectral range (250 - 4000) cm^{-1}. A number of 512 scans are typically used for these measurements. Before each series of measurements, a pellet of pure KBr (0.2 g) is used as a reference for the subtraction of the bottom line of the final spectra of the K

powders.

2.3.4. Thermogravimetric Analysis (TGA)

Thermogravimetric analysis (TGA) consists of heating a sample under a controlled atmosphere and determining its mass loss as a function of temperature. The TGA analyses of the various K powders were carried out using the TGA-Q500 system (Thermal Advantages of the company TA-Instruments). For a typical TG analysis, 5 mg of K powder is placed in a small flat cuvette made of platinum (Pt). The latter is then introduced into the vertical oven, where an air flow of 60 mL/min circulates. The temperature range studied is between room temperature (25˚C) and 1000˚C. The heating rate is fixed at 10˚C/min. The mass loss curves as a function of temperature are differentiated with respect to temperature to bring out the transition peaks corresponding to mass losses and/or phase changes.

2.3.5. Scanning Electron Microscopy (SEM) Analysis

The scanning electron microscope (SEM) is a device that uses high-voltage accelerated electron beams to observe sample surface morphology at the microscopic (or even nanometric) scale. SEM analysis of the different K powders was carried out using a VEGA3 system (TESCAN) with an electron source subjected to a high voltage fixed at 20 kV. The system is equipped with a Tescan Low Vaccum Secondary Electron Detector (LVSTD). For analysis purposes, the samples are installed on a sample holder which itself is introduced into the SEM enclosure where a vacuum of 5×10^{-2} Pa must be maintained (using a pumping bench primary and turbo-molecular) to be able to carry out SEM observations.

2.3.6. Energy Dispersive X-Ray Spectroscopy (EDX) Analysis

Analysis by energy dispersive X-ray spectroscopy (EDX) was done in the same SEM system and used the same beam of accelerated electrons at high voltage (20 kV), except that the major difference concerned the X-rays produced by the incident electron beam. It is thus possible to characterize the composition of a sample from its X-ray emission fingerprint. The EDX analysis of the different K powders was carried out with the same VEGA3 system (TESCAN) composed of a source of electrons (accelerated to 20 kV) and an X-ray detector (XFlash, Bruker).

3. Results and Discussion

3.1. pH Determination

The pH of the samples is slightly acidic as shown by the values in **Table 1**. pH values range from 5.70 to 6.26 and are similar to those of a previous study [10]. This acidic pH would be due to minerals matter. According to ICP-OES analysis we found more oxides on the clays.

3.2. Materials Characterization

3.2.1. ICP-OES Analysis

The results of chemical analysis by ICP-OES are recorded in **Table 2** (major

Table 1. pH measurement of the different samples.

Samples	pH
K1	5.74
K2	5.84
K3	5.74
K4	5.70
K5	5.75
K6	6.26
K7	6.25

Table 2. Chemical composition of the samples expressed in percentage by mass of major elements.

Parameters \ Samples	K1	K2	K3	K4	K5	K6	K7
SiO_2	47.2	45.2	51.4	54.0	52.8	53.3	65.3
Al_2O_3	23.7	19.2	21.3	22.9	23.3	17.7	14.9
Fe_2O_3	15.3	14.9	10.6	9.9	11.8	11.9	6.43
MnO	0.034	0.266	0.038	0.098	0.032	0.084	0.028
MgO	0.34	1.67	1.61	0.99	0.16	1.53	0.68
CaO	<0.002	0.27	0.022	0.033	0.003	1.66	0.57
Na_2O	0.06	0.11	0.08	0.098	0.032	0.084	0.028
K_2O	0.75	0.68	1.32	2.40	1.14	1.13	1.03
TiO_2	1.02	1.03	0.95	0.92	0.96	0.95	0.66
P_2O_5	0.03	0.02	0.05	0.03	0.05	0.04	0.03
S	0.025	0.029	0.033	0.020	0.027	0.025	0.028
Fire loss	10.8	14.5	14.2	8.7	8.7	9.9	6.2

elements) and **Table 3** (minor elements). The clays studied are characterized by:

- A comparable loss on ignition for samples K1, K2 and K3, but it is lower for sample K7, which confirms its siliceous nature in agreement with a previous study carried out in Tunisia [11];
- Contents of silica SiO_2, alumina Al_2O_3 and iron oxide Fe_2O_3 for all samples (K1 to K7) similar to Katiola clay [12].

The determination of minor elements shows the absence of arsenic, cadmium and lead in all materials. Moreover, clay samples contain chromium (873 to 150 ppm), barium (676 to 143 ppm), nickel (450 to 40 ppm), zirconium (320 to 111 ppm), strontium (276 to 11.4 ppm), zinc (257 to 23 ppm), vanadium (242 to 105 ppm), copper (154 to 38 ppm), lanthanum (85 to 26 ppm), cobalt (78 to 6 ppm), yttrium (54.2 to 16.1 ppm) and scandium (46.9 to 13.9 ppm).

Table 3. Chemical composition of the samples expressed in ppm in minor elements.

Parameters \ Samples	K1	K2	K3	K4	K5	K6	K7
Arsenic: As	<30	<30	<30	<30	<30	<30	<30
Barium: Ba	143	676	256	534	213	389	302
Cadmium: Cd	<1.5	<1.5	<1.5	<1.5	<1.5	<1.5	<1.5
Cobalt: Co	16	78	25	24	6	39	12
Chromium: Cr	218	873	150	150	135	208	181
Copper: Cu	107	154	89	70	39	137	38
Lanthanum: La	26	57	39	41	30	85	39
Molybdenum: Mo	5	10	<3	5	5	4	5
Nickel: Ni	50	450	68	70	40	80	66
Lead: Pb	<30	<30	<30	<30	<30	<30	<30
Scandium: Sc	35.5	46.9	30.7	25.0	21.0	28.2	13.9
Strontium: Sr	11.4	50.3	12.4	27.4	33.1	276	148
Vanadium: V	242	190	190	152	180	190	105
Yttrium: Y	16.1	39.5	22.0	29.0	16.4	54.2	20.0
Zinc: Zn	52	257	121	74	23	88	45
Zirconium: Zr	240	166	170	200	320	111	200

3.2.2. TG Analysis

The derivative thermogravimetric analysis (DTG) curves obtained (**Figure 2**) look the same and show all the phenomena characteristic of kaolin-type clays [13] [14] which are:

- An endothermic peak around 50˚C corresponding to the loss of absorbed water;
- An exothermic peak centered at 450˚C due to the dehydroxylation of kaolinite towards the formation of a non-crystalline phase (meta-kaolinite), indicating the loss of constitution water (450˚C - 650˚C).

3.2.3. X-Ray Diffraction Analysis

Figure 3 presents the X-ray diffraction patterns of the samples, showing different intensity peaks. The major crystalline phases detected are mainly made up of:

- $Si_2O_5Al_2(OH)_4$ kaolinite (peaks at 12.5 Å; 20 Å; 24.9 Å; 34.9 Å; 38.2 Å; 39 Å; 62.5 Å) in the majority of the samples (K1 to K7);
- Muscovite (lines at 8.9 Å; 17.8 Å) for samples K4, K5 and K6;
- Smectite (lines at 6 Å; 29 Å; 36.8 Å) for samples K2 and K6;
- Quartz SiO_2 as impurity (lines at 21 Å; 26 Å; 39.5 Å; 50 Å; 60 Å) for all samples (K1 to K7).

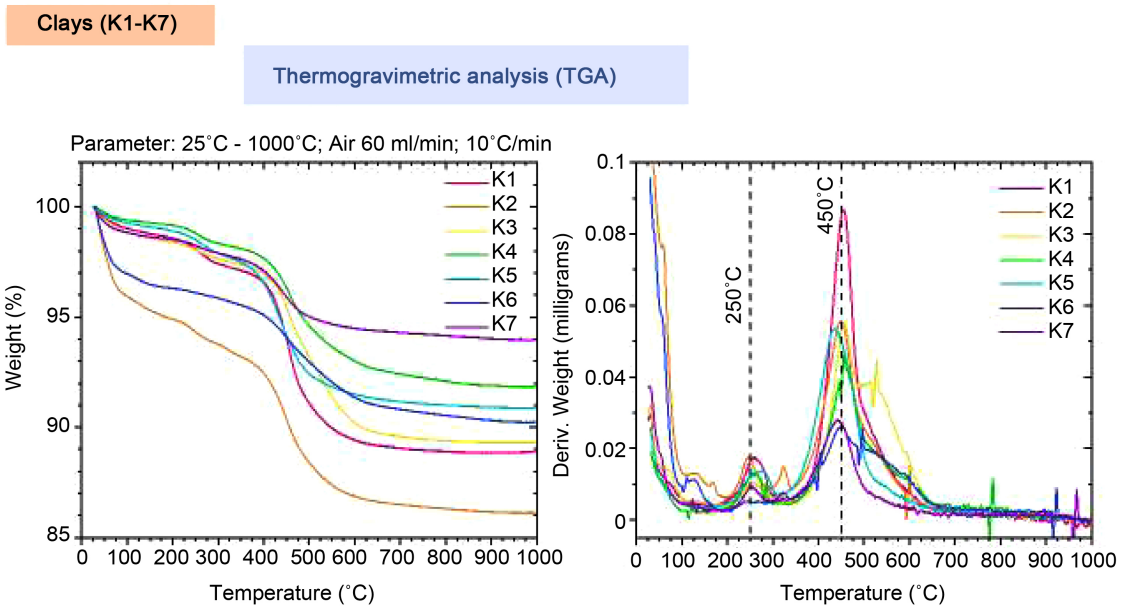

Figure 2. Derivative thermogravimetric analysis curves of clay samples.

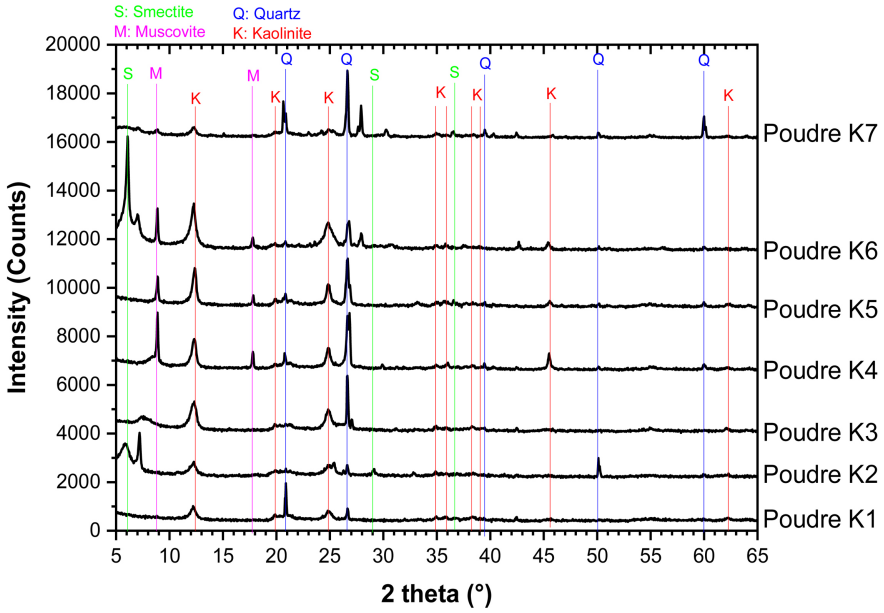

Figure 3. X-ray diffraction patterns of clay samples.

3.2.4. FTIR Analysis

The infrared spectra are almost similar (**Figure 4**) and include the following absorption bands:

- Between 3750 and 3500 cm^{-1}, the bands observed are those of the elongation of the hydroxyls; those at 3695; 3652 and 3618 cm^{-1} are characteristic of the valence vibrations of the OH groups of kaolinite [15] [16];
- Between 1200 and 700 cm^{-1}, Si-O stretching vibrations are observed. The band at 1112 cm^{-1} is the characteristic band of kaolinite. The shoulders at 693 and 788 cm^{-1} can be attributed to the presence of quartz [17];

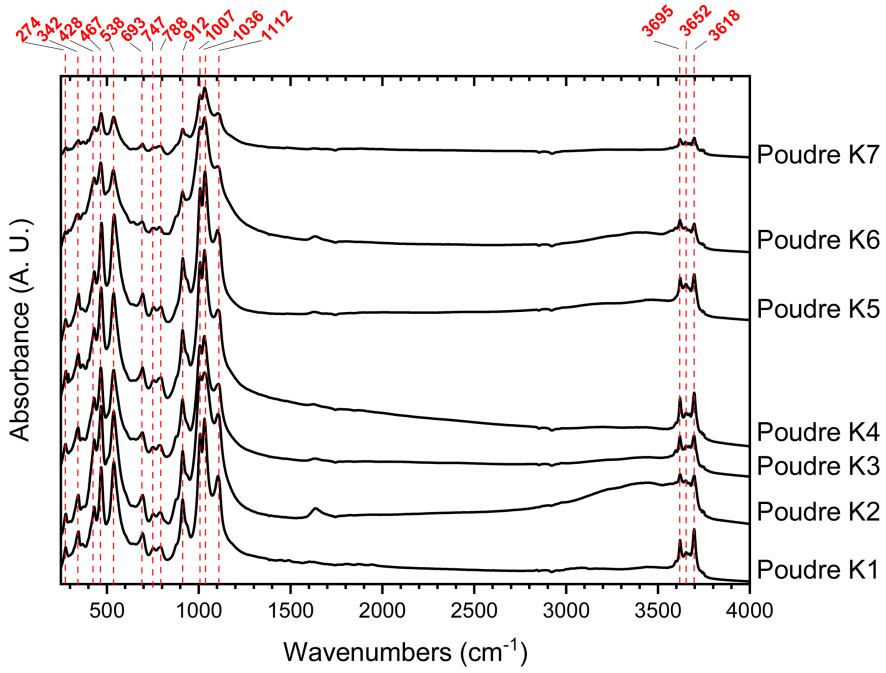

Figure 4. Infrared spectra of clay samples.

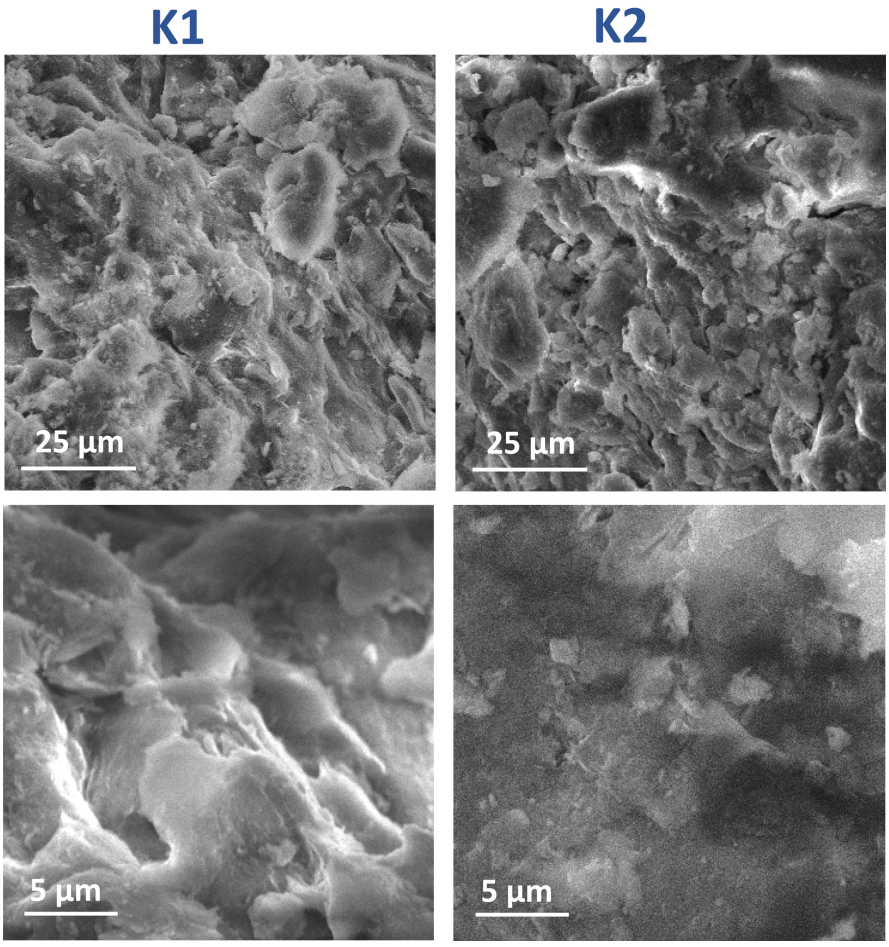

Figure 5. Samples K1 and K2 SEM images.

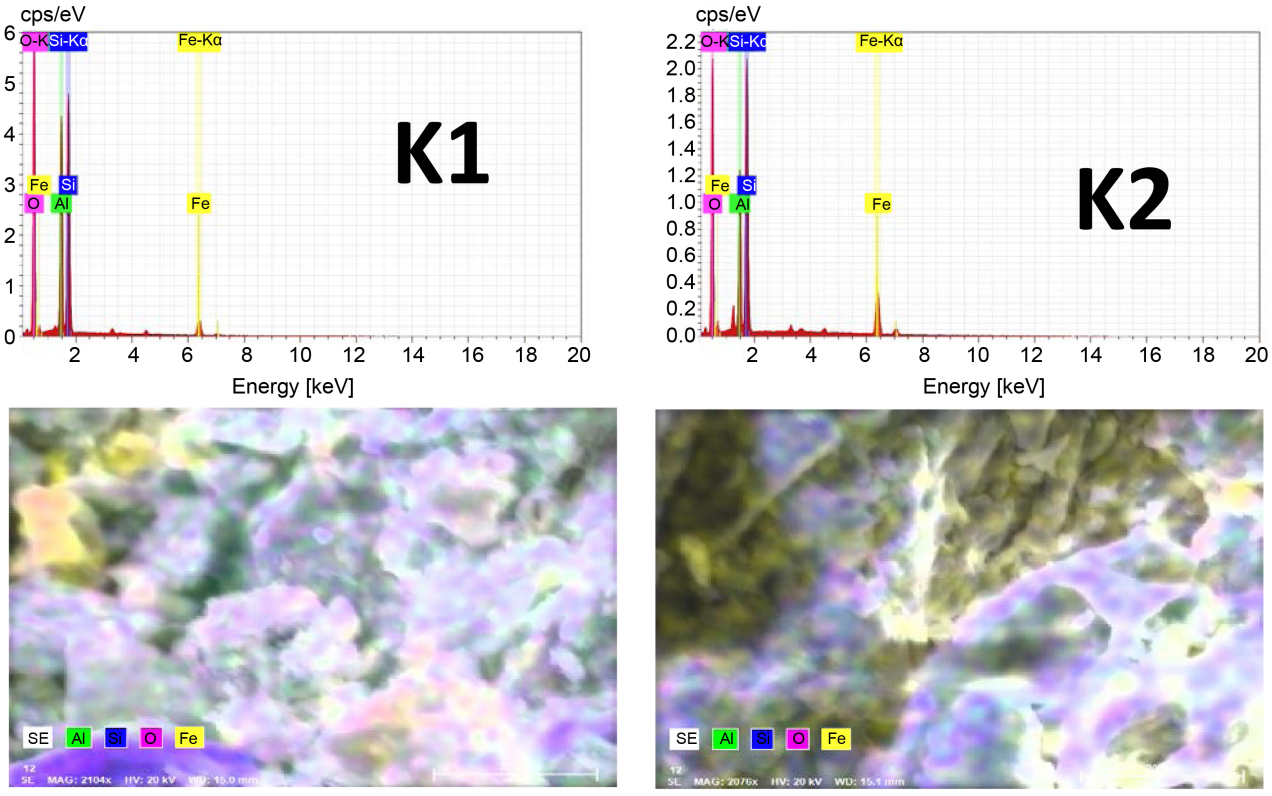

Map

Element	At. No.	Netto	Mass [%]	Mass Norm. [%]	Atom [%]	abs. error [%] (1 sigma)	rel. error [%] (1 sigma)
Aluminium	13	64482	13.69	15.70	11.59	0.68	5.00
Silicon	14	78356	16.31	18.70	13.27	0.72	4.45
Oxygen	8	71869	50.76	58.23	72.51	5.89	11.60
Iron	26	8905	6.42	7.37	2.63	0.22	3.40
		Sum	87.18	100.00	100.00		

Map

Element	At. No.	Netto	Mass [%]	Mass Norm. [%]	Atom [%]	abs. error [%] (1 sigma)	rel. error [%] (1 sigma)
Aluminium	13	18232	9.39	12.90	10.04	0.49	5.19
Silicon	14	34051	16.39	22.50	16.83	0.74	4.49
Oxygen	8	25647	37.97	52.14	68.45	4.81	12.66
Iron	26	9240	9.07	12.46	4.68	0.30	3.26
		Sum	72.82	100.00	100.00		

Figure 6. Samples K1 and K2 EDX images.

- Between 950 and 600 cm^{-1}, the Al-OH deformation vibrations appear, the band of which at 912 cm^{-1} is characteristic of kaolinite [17];
- At 1036 cm^{-1}, a Si-O-Si stretching vibration characteristic of kaolinite [15] is observed;
- At 1007 and 538 cm^{-1}, a Si-O-Al stretching vibration characteristic of kaolinite [15] is observed;
- At 428 cm^{-1} a deformation vibration of the Si-O or Al-O bonds can be suspected.

3.2.5. SEM Analysis

Scanning electron microscope observation of the samples (**Figure 5**) revealed:

- The presence of smectite in the form of piles in superimposed sheets with undulations [18];
- Plane and sub-hexagonal crystalline forms corresponding to kaolinite [19];
- The presence of quartz grains embedded in the matrix [19];
- The presence of muscovite in the form of flakes [20].

3.2.6. Chemical Composition and Energy Dispersive X-Ray Spectroscopy (EDX) Elemental Mapping

The different EDX spectra (**Figure 6**) show the presence of elements such as silica, aluminum and iron in the different clay samples analyzed. These results are similar to those of some authors, with different composition percentages [21] [22].

4. Conclusion

Physical, chemical and mineralogical analyses of raw clay materials from the Katiola quarries were carried out. The chemical characterization indicates that the seven samples collected contain substantially the same chemical elements with almost identical proportions. They mainly contain silica SiO_2, alumina Al_2O_3 and iron oxide Fe_2O_3. XRD, FT-IR and SEM-EDX analyses confirmed the presence of kaolinite, muscovite, smectite and quartz.

Conflicts of Interest

The authors declare no conflicts of interest regarding the publication of this paper.

References

[1] Traoré, K., Blanchart, P., Jernot, J.P. and Gomina, M. (2007) Caractérisation Physicochimique et Mécanique de Matériaux Céramiques Obtenus à Partir d'une Argile Kaolinitique du Burkina Faso. *Comptes Rendus Chimie*, **10**, 511-517. https://doi.org/10.1016/j.crci.2006.12.009

[2] Bagal, M. and Vittori, M. (2010) Les Indications Géographiques en Côte d'Ivoire, Produits Potentiels et Cadre Juridique Pertinent. Paper Commissioned by the ACP-EU TradeCom Facility in the Context of the ACP Regional Workshops on Geographical Indications.

[3] Kedi, A.B.B., Kouassi, S.S., Coulibaly, V. and Sei, J. (2021) Élimination de Polluants des Déchets Liquides d'une Unité de Production de Sucre par des Argiles Naturelles de Côte d'Ivoire. *International Journal of Biological and Chemical Sciences*, **15**, 803-815. https://doi.org/10.4314/ijbcs.v15i2.31

[4] Yao, K.N., Goovaerts, T., Leduc, T., Kouassi, K.S. and Goemaere, E. (2017) Contribution à l'Analyse de la Production Céramique de la Région de Gbèkè dans le Centre de la Côte d'Ivoire. *Nyame Akuma*, **88**, 8-15.

[5] Watanabe, Y. (1963) Étude des Argiles dans les Sols au Microscope Electronique. *Soil Science and Plant Nutrition*, **9**, 6-10. https://doi.org/10.1080/00380768.1963.10431041

[6] Truche, C. (2010) Caractérisation et Quantification des Minéraux Argileux dans les Sols Expansifs par Spectroscopie Infrarouge aux Echelles du Laboratoire et du Terrain. Master's Thesis, Université Paul Sabatier-Toulouse III, Toulouse.

[7] Amin, N., Andji, Y.Y.J., Aké, M. and Yolou, S. (2009) Minéralogie et Physicochimie d'Argiles de Traitement de L'ulcère de Buruli en Côte d'Ivoire. *Journal des Sciences Pharmaceutiques et Biologiques*, **10**, 21-30.

[8] Koriko, M., Zounon, D., Bafai, D.D., Tchegueni, S., Degbe, K.A., Fiaty, K., Drogui, P. and Tchangbedji, G. (2021) Formulation and Characterization of Light Aggregates

from Phosphate Ore Processing Waste from the Hahotoe and Kpogame Mines, Potential Use for Agricultural Applications. *Journal of Minerals and Materials Characterization and Engineering*, **9**, 390-405.
https://doi.org/10.4236/jmmce.2021.94027

[9] Koriko, M., Zounon, D., Degbe, A., Tchegueni, S., Dihéénane, D.B., Fiaty, K., Tchangbedji, G. and Drogui, P.(2021) Caractérisations Physico-Chimiques et Minéralogiques ee l'Argile d'Aklakou Utilisée dans la Poterie en Vue de son Application dans la Formulation des Agrégats Légers. *International Journal of Advanced Research*, **9**, 706-712. https://doi.org/10.21474/IJAR01/13471

[10] Soro, D., Bakayoko, S., Dao, D., Trabi, T., Angui, P. and Girardin, O. (2011) Diagnostic de Fertilité du Sol au Centre-Nord de la Côte d'Ivoire. *Agronomie Africaine*, **23**, 205-215.

[11] Elfil, H., Srasra, E. and Dogguy, M. (1995) Caractérisation Physico-Chimique de Certaines Argiles Utilisées dans l'Industrie Céramique. *Journal of Thermal Analysis*, **44**, 663-683. https://doi.org/10.1007/BF02636285

[12] Kouadio, L.M., El Islam Lebouachera, S., Blanc, S., Sei, J., Miqueu, C., Pannier, F. and Martinez, H. (2022) Characterization of Clay Materials from Ivory Coast for Their Use as Adsorbents for Wastewater Treatment. *Journal of Minerals and Materials Characterization and Engineering*, **10**, 319-337.
https://doi.org/10.4236/jmmce.2022.104023

[13] Jouenne, C.A. (1990) Traité de Céramique et Matériaux Minéraux. Ed. Septima, Paris.

[14] Mackenzie, R.C. (1957) Mineralogical Society (Great Britain). The Differential Thermal Investigation of clays. Mineralogical Society, London.

[15] Farmer, V.C. (1974) The Infrared Spectra of Minerals. Mineralogical Society, London. https://doi.org/10.1180/mono-4

[16] Prost, R. (1989) Infrared Study of Structural OH in Kaolinite, Dickite, Nacrite, and Poorly Crystalline Kaolinite at 5 to 600 K. *Clays and Clay Minerals*, **37**, 464-468.
https://doi.org/10.1346/CCMN.1989.0370511

[17] Wilson, M.J. (1994) Clay Mineralogy: Spectroscopic and Chemical Determinative Methods. Chapman & Hall, London. https://doi.org/10.1007/978-94-011-0727-3

[18] Lazzez, M. (2006) Étude Diagénétique des Argiles et Caractérisation d'Altération Hydrothermale. *International Conference Geologies Arab World* (*GAW*8), Giza, 13-16 February 2006, 417-423.

[19] Hattab, M., Bouziri-Adrouche, S. and Fleureau, J.M. (2010) Évolution de la Microtexture d'une Matrice Kaolinitique sur Chemin Triaxial Axisymétrique. *Canadian Geotechnical Journal*, **47**, 34-48. https://doi.org/10.1139/T09-098

[20] Huyen, D.T., Tabelin, C.B., Thuan, H.M., Dang, D.H., Truong, P.T. and Vongphuthone, B. (2019) Geological and Geochemical Characterizations of Sediments in Six Borehole Cores from the Arsenic-Contaminated Aquifer of the Mekong Delta, Vietnam. *Data Brief*, **25**, Article ID: 104230.
https://doi.org/10.1016/j.dib.2019.104230

[21] Benjelloun, Y., Miyah, Y., Idrissi, M., Boumchita, S., Lahrichi, A. and Lalami, A.E.O. (2016) Étude de la Performance Catalytique Pendant l'Oxydation du Bleu de Méthylène en Utilisant un Catalyseur MnO-Argile en Présence de H_2O_2. *Journal of Materials and Environmental Science*, **7**, 9-17.

[22] Guerraoui, F., Zamama, M. and Ibnoussina, M. (2009) Thermal Behaviour of the Ceramic and Pottery of Safi-Morocco. *Physical and Chemical News*, **49**, 114-120.